Oleg Bogoyavlenskij*

New Exact Axisymmetric Solutions to the Navier–Stokes Equations

https://doi.org/10.1515/zna-2019-0262
Received August 7, 2019; accepted October 27, 2019; previously published online November 23, 2019

Abstract: Infinite-dimensional space of axisymmetric exact solutions to the Navier–Stokes equations with time-dependent viscosity $\nu(t)$ is constructed. Inner transformations of the exact solutions are defined that produce an infinite sequence of new solutions from each known one. The solutions are analytic in the whole space $\mathbb{R}^3$ and are described by elementary functions. The bifurcations of the instantaneous (for $t = t_0$) phase portraits of the viscous fluid flows are studied for the new exact solutions. Backlund transforms between the axisymmetric Helmholtz equation and a linear case of the Grad–Shafranov equation are derived.

Keywords: Backlund Transforms; Collapses; Discontinuous Functions; Inner Transformations; Viscous Flows; Vortex Blobs; Vortex Rings.

1 Introduction

Different aspects of theory of Navier–Stokes equations were developed in numerous publications (see [1–5] and references therein). During the past 190 years, many exact solutions to the Navier–Stokes equations (1823) were derived. There are several reviews devoted to the exact solutions possessing different symmetries [6–10].

We introduce in this article new axisymmetric time-dependent exact solutions to the Navier–Stokes equations. The solutions are studied in the cylindrical coordinates r, z, φ and depend on variables r, z, and time t. We construct an infinite-dimensional space of solutions for which fluid velocity $\mathbf{V}(r, z, t)$ is analytic in the whole space $\mathbb{R}^3$ and is defined for all moments of time t. Inner transformations acting on the space of exact solutions are presented that generate from any exact solution an infinite sequence of new ones.

We study the bifurcations of the instantaneous (for $t = t_0$) phase portraits of the viscous fluid flows for the new exact solutions. Namely, we investigate dynamics of the vortex blobs and vortex rings, which are the maximal compact domains invariant (for any fixed moment of time t_0) with respect to the vorticity vector field $\nabla \times \mathbf{V}(r, z, t_0)$. As known, for the ideal incompressible fluid, the vorticity field is frozen into the fluid flow. Therefore, the vortex blobs and vortex rings are transported with the ideal fluid flow; their volume is constant. We show that for the constructed exact solutions to the Navier–Stokes equations, the vortex blobs and vortex rings are not frozen into the viscous fluid flow and collapse and disappear as $t \to \infty$.

For the new exact solutions, we study the behaviour of the volume $V_m(t)$ of the vortex blob. We show that despite the analyticity of exact solutions the function $V_m(t)$ is not even continuous. The function $V_m(t)$ is a discontinuous monotonously decreasing function of time t that has jumps down and infinite derivatives at an infinite sequence of moments of time $-\infty < \cdots < t_k < \cdots < t_3 < t_2 < t_m$, where $t_k \to -\infty$ when $k \to \infty$. The volume function $V_m(t)$ has its minimal value at $t = t_m$. Function $V_m(t)$ is defined for $t \in (-\infty, t_m)$. Here, t_m is the maximal time when the vortex blob exists; it does not exist for $t > t_m$.

2 Infinite-Dimensional Space of Exact Solutions

I. In this article, we derive and study new exact solutions to the Navier–Stokes equations

$$\frac{\partial \mathbf{V}}{\partial t} + (\mathbf{V} \cdot \nabla)\mathbf{V} = -\frac{1}{\rho}\nabla p + \nabla \Psi + \nu \Delta \mathbf{V},$$
$$\nabla \cdot \mathbf{V} = 0, \tag{1}$$

where $\mathbf{V}(\mathbf{x}, t)$ is the fluid velocity; $p(\mathbf{x}, t)$, the pressure; ρ, a constant density; $\Psi(\mathbf{x}, t)$, an arbitrary gravitational potential; $\nu(t)$, the kinematic viscosity that is an arbitrary piecewise continuous nonnegative function of time t; and Δ, the Laplace operator.

Theorem 1: *The Navier–Stokes equations* (1) *have exact z-axisymmetric solutions*

$$\mathbf{V}(r, z, t) = \alpha \xi r \hat{\mathbf{e}}_\varphi + 2\xi \hat{\mathbf{e}}_z + f(t)\mathbf{B}(r, z), \tag{2}$$

***Corresponding author: Oleg Bogoyavlenskij,** Queen's University, Kingston, Ontario, Canada, E-mail: Bogoyavl@mast.queensu.ca

$$p(r,z,t)=\rho\Big[C+\Psi(r,z,t)+\alpha^2\xi^2r^2 +\alpha^2\xi f(t)\psi(r,z)-\frac{1}{2}|\mathbf{V}(r,z,t)|^2\Big], \quad (3)$$

where α, ξ, and C are arbitrary constant parameters; $\hat{\mathbf{e}}_r$, $\hat{\mathbf{e}}_z$, $\hat{\mathbf{e}}_\varphi$ are the unit vector fields tangent to the cylindrical coordinates r, z, φ. The function of time $f(t)$ is

$$f(t)=\exp\left(-\alpha^2\int_0^t \nu(\tau)d\tau\right). \quad (4)$$

The z-axisymmetric vector fields $\mathbf{B}(r,z)$ are steady and have the form

$$\mathbf{B}(r,z)=-\frac{1}{r}\frac{\partial\psi}{\partial z}\hat{\mathbf{e}}_r+\frac{1}{r}\frac{\partial\psi}{\partial r}\hat{\mathbf{e}}_z+\frac{\alpha\psi}{r}\hat{\mathbf{e}}_\varphi, \quad (5)$$

where the streamfunction $\psi(r,z)$ is an arbitrary solution to the equation

$$\frac{\partial^2\psi}{\partial r^2}-\frac{1}{r}\frac{\partial\psi}{\partial r}+\frac{\partial^2\psi}{\partial z^2}=-\alpha^2\psi. \quad (6)$$

The vector fields $\mathbf{B}(r,z)$ (5)–(6) satisfy the Beltrami equation

$$\nabla\times\mathbf{B}(\mathbf{x})=\alpha\mathbf{B}(\mathbf{x}). \quad (7)$$

If for some period of time $c\le t\le d$ viscosity $\nu(t)=0$, then solution (2), (3) becomes a steady solution for $c\le t\le d$ to the Euler equations for ideal incompressible fluid dynamics.

Proof. (*a*) The vorticity field for the vector field (5) has the form

$$\nabla\times\mathbf{B}(r,z)=-\frac{\alpha}{r}\frac{\partial\psi}{\partial z}\hat{\mathbf{e}}_r+\frac{\alpha}{r}\frac{\partial\psi}{\partial r}\hat{\mathbf{e}}_z -\frac{1}{r}\left(\frac{\partial^2\psi}{\partial r^2}-\frac{1}{r}\frac{\partial\psi}{\partial r}+\frac{\partial^2\psi}{\partial z^2}\right)\hat{\mathbf{e}}_\varphi. \quad (8)$$

Substituting here (6), we arrive at the Beltrami equation (7).

As a consequence of (7), we get $\nabla\cdot\mathbf{B}=0$. As $r\hat{\mathbf{e}}_\varphi=-y\hat{\mathbf{e}}_x+x\hat{\mathbf{e}}_y$, the vector fields $\mathbf{V}(r,z,t)$ (2) also satisfy the incompressibility equation $\nabla\cdot\mathbf{V}=0$.

(*b*) Let us show that vector fields $\mathbf{V}(r,z,t)$ (2) satisfy equation

$$(\nabla\times\mathbf{V})\times\mathbf{V}=\nabla\Big[-\alpha^2\xi^2r^2-\alpha^2\xi f(t)\psi(r,z)\Big]. \quad (9)$$

Indeed, using equation

$$\nabla\times\left[\alpha\xi r\hat{\mathbf{e}}_\varphi+2\xi\hat{\mathbf{e}}_z\right]=2\alpha\xi\hat{\mathbf{e}}_z \quad (10)$$

and (7), we find for the vector fields $\mathbf{V}(r,z,t)$ (2):

$$\nabla\times\mathbf{V}(r,z,t)=2\alpha\xi\hat{\mathbf{e}}_z+\alpha f(t)\mathbf{B}(r,z) =\alpha\mathbf{V}(r,z,t)-\alpha^2\xi r\hat{\mathbf{e}}_\varphi. \quad (11)$$

The equation proves that vector fields $\mathbf{V}(r,z,t)$ (2) for $\xi\neq0$ are not the Beltrami fields. Equation (11) yields

$$(\nabla\times\mathbf{V})\times\mathbf{V}=\left(\alpha\mathbf{V}-\alpha^2\xi r\hat{\mathbf{e}}_\varphi\right)\times\mathbf{V} =-\alpha^2\xi r\hat{\mathbf{e}}_\varphi\times\mathbf{V}. \quad (12)$$

Applying to (12) the identities $\hat{\mathbf{e}}_\varphi\times\hat{\mathbf{e}}_z=\hat{\mathbf{e}}_r$, $\hat{\mathbf{e}}_\varphi\times\hat{\mathbf{e}}_r=-\hat{\mathbf{e}}_z$, $\hat{\mathbf{e}}_\varphi\times\hat{\mathbf{e}}_\varphi=0$ and (2), (5), we find

$$\begin{aligned}(\nabla\times\mathbf{V})\times\mathbf{V}&=(-\alpha^2\xi r\hat{\mathbf{e}}_\varphi)\times\Big[\alpha\xi r\hat{\mathbf{e}}_\varphi+2\xi\hat{\mathbf{e}}_z\\ &\quad+f(t)\Big(-\frac{1}{r}\frac{\partial\psi}{\partial z}\hat{\mathbf{e}}_r+\frac{1}{r}\frac{\partial\psi}{\partial r}\hat{\mathbf{e}}_z+\frac{\alpha\psi}{r}\hat{\mathbf{e}}_\varphi\Big)\Big]\\ &=-2\alpha^2\xi^2r\hat{\mathbf{e}}_r-\alpha^2\xi f(t)\left[\frac{\partial\psi}{\partial r}\hat{\mathbf{e}}_r+\frac{\partial\psi}{\partial z}\hat{\mathbf{e}}_z\right]\\ &=\nabla\Big[-\alpha^2\xi^2r^2-\alpha^2\xi f(t)\psi(r,z)\Big]. \end{aligned} \quad (13)$$

(*c*) Using the well-known identity

$$(\mathbf{V}\cdot\nabla)\mathbf{V}=(\nabla\times\mathbf{V})\times\mathbf{V}+\nabla\left(\frac{1}{2}|\mathbf{V}|^2\right)$$

and (13), we present the Navier–Stokes equations (1) in the form

$$\frac{\partial\mathbf{V}}{\partial t}=-\nabla\left[\frac{1}{\rho}p-\Psi-\alpha^2\xi^2r^2-\alpha^2\xi f(t)\psi(r,z)+\frac{1}{2}|\mathbf{V}|^2\right] +\nu(t)\Delta\mathbf{V}. \quad (14)$$

Applying to the identity $\Delta\mathbf{B}=\nabla(\nabla\cdot\mathbf{B})-(\nabla\times)(\nabla\times\mathbf{B})$ the Beltrami equation (7) and equation $\nabla\cdot\mathbf{B}=0$, we derive $\Delta\mathbf{B}=-\alpha^2\mathbf{B}$. Formula $r\hat{\mathbf{e}}_\varphi=-y\hat{\mathbf{e}}_x+x\hat{\mathbf{e}}_y$ implies $\Delta(\alpha\xi r\hat{\mathbf{e}}_\varphi+2\xi\hat{\mathbf{e}}_z)=0$. Therefore, for the vector field $\mathbf{V}(r,z,t)$ (2), we find

$$\Delta\mathbf{V}=\Delta\left[\alpha\xi r\hat{\mathbf{e}}_\varphi+2\xi\hat{\mathbf{e}}_z+f(t)\mathbf{B}\right]=f(t)\Delta\mathbf{B} =-\alpha^2f(t)\mathbf{B}. \quad (15)$$

Substituting formulas (2) and (15) into the Navier–Stokes equation (14), we transform it to the form

$$\begin{aligned}&\frac{\partial\left[\alpha\xi r\hat{\mathbf{e}}_\varphi+2\xi\hat{\mathbf{e}}_z+f(t)\mathbf{B}\right]}{\partial t}\\ &=-\nabla\left[\frac{1}{\rho}p-\Psi-\alpha^2\xi^2r^2-\alpha^2\xi f(t)\psi(r,z)+\frac{1}{2}|\mathbf{V}|^2\right]\\ &\quad-\alpha^2\nu(t)f(t)\mathbf{B}. \end{aligned} \quad (16)$$

Inserting here formula (3) for the pressure $p(r, z, t)$, we find that (16) is reduced to equation

$$\frac{\mathrm{d}f(t)}{\mathrm{d}t} = -\alpha^2 \nu(t) f(t) \tag{17}$$

that is identically satisfied by the function $f(t)$ (4).

(*d*) If $\nu(t) = 0$ for $c \le t \le d$, then Navier–Stokes equations (1) become Euler equations for ideal incompressible fluid. Equation (17) yields $f(t) = \text{const}$ for $c \le t \le d$. Hence, solutions (2), (3) for $c \le t \le d$ become steady solutions to the Euler equations.

Analogously, if viscosity $\nu(t) = 0$ on two intervals of time $c \le t \le d$ and $c_1 \le t \le d_1$ and $\nu(t) > 0$ for $d < t < c_1$, then solution (2), (3) describes transition of viscous fluid between two steady flows of inviscid fluid for $c \le t \le d$ and $c_1 \le t \le d_1$. □

Remark 1: The new exact solutions (2), (3) depend on the infinite-dimensional family of axisymmetric Beltrami fields $\mathbf{B}(r, z)$ (5) and (6) and on two arbitrary parameters α and ξ. Therefore, Theorem 1 presents an infinite-dimensional space $\mathcal{L}_\alpha$ of exact solutions to the Navier–Stokes equations (1).

Remark 2: After changing parameter α to $(-\alpha)$ in the exact solution (2), (3), one gets the exact viscous flow having the opposite rotation around the axis z.

Remark 3: Using results of our article [11], we get that the z-axisymmetric Beltrami vector fields $\mathbf{B}(r, z)$ (5) to (7) admit the integral representation

$$\mathbf{B}(\mathbf{x}) = \int\limits_{S^2} \big[\sin(\alpha \mathbf{k}\cdot\mathbf{x})\mathbf{T}(\mathbf{k}) + \cos(\alpha \mathbf{k}\cdot\mathbf{x})\mathbf{k}\times\mathbf{T}(\mathbf{k})\big]\mathrm{d}\sigma. \tag{18}$$

Here, $\mathbf{T}(\mathbf{k})$ is an arbitrary z-axisymmetric differentiable vector field tangent to the unit sphere S^2: $\mathbf{k}\cdot\mathbf{k} = 1$, and $\mathrm{d}\sigma$ is the standard Euclidean measure on the sphere S^2. Indeed, in [11], we proved that the general nonsymmetric solution to the Beltrami equation (7) has form (18), where $\mathbf{T}(\mathbf{k})$ is an arbitrary vector field tangent to the sphere S^2, and $\mathrm{d}\sigma$ is an arbitrary measure on S^2. The Beltrami field $\mathbf{B}(\mathbf{x})$ (18) evidently becomes z-axisymmetric if the vector field $\mathbf{T}(\mathbf{k})$ and the measure $\mathrm{d}\sigma$ are z-axisymmetric. As we have shown in [11], the absolute value $|\mathbf{B}(\mathbf{x})|$ decreases as $C/|\mathbf{x}|$ when $|\mathbf{x}| \to \infty$; see also [12].

Remark 4: The solutions (2), (3) exist for all moments of time $t \in (-\infty, \infty)$. Below we assume that viscosity $\nu(t) \ge \nu_0 > 0$; for this case, function $f(t)$ (4) monotonously decreases and $f(t) \to \infty$ at $t \to -\infty$ and $f(t) \to 0$ at $t \to \infty$. Therefore, (2) yields that the exact solutions at $t \to \infty$ tend to the steady flow

$$\tilde{\mathbf{V}}(r, z) = \alpha\xi r\hat{\mathbf{e}}_\varphi + 2\xi\hat{\mathbf{e}}_z, \tag{19}$$

that according to (10) has constant vorticity $\nabla\times\tilde{\mathbf{V}}(r, z) = 2\alpha\xi\hat{\mathbf{e}}_z$. Therefore, solutions (2) describe a relaxation of the axisymmetric flows (2) to the steady flow (19) with constant vorticity $2\alpha\xi\hat{\mathbf{e}}_z$.

Solutions (2) at $t \to -\infty$ have the leading term $f(t)\mathbf{B}(r, z)$ which describes a Beltrami flow with the streamfunction $f(t)\psi(r, z)$.

3 Infinite-Dimensional Family of Inner Transformations

Theorem 2: *If two axisymmetric vector fields* $\mathbf{V}_1(r, z, t)$ *and* $\mathbf{V}_2(r, z, t)$ *are solutions of form* (2) *to the Navier–Stokes equations* (1)*, then vector fields*

$$\begin{aligned}
&\mathbf{V}_{MN}(r, z, t)\\
&\quad= \sum_{n=1}^{M} a_{1n}\mathbf{V}_1(r, z + u_{1n}, t)\\
&\qquad+ \sum_{n=1}^{M} a_{2n}\mathbf{V}_2(r, z + u_{2n}, t) + \alpha\xi r\hat{\mathbf{e}}_\varphi\\
&\qquad+ 2\xi\hat{\mathbf{e}}_z + \sum_{k=1}^{N}\sum_{n=1}^{M}\Big[b_{kn}\frac{\partial^n\mathbf{V}_1(r, z + z_{kn}, t)}{\partial z^n}\\
&\qquad+ c_{kn}\frac{\partial^n\mathbf{V}_2(r, z + \tilde{z}_{kn}, t)}{\partial z^n}\Big]
\end{aligned} \tag{20}$$

also are solutions to the Navier–Stokes equations (1)*. The constants* a_{jn}, u_{jn} $(j = 1, 2)$, b_{kn}, c_{kn}, z_{kn}, $\tilde{z}_{kn}$ *are arbitrary,* $n = 1, \cdots, M$, $k = 1, \cdots, N$.

Proof. Let vector fields $\mathbf{V}_j(r, z, t)$ (2) $(j = 1, 2)$ are as follows:

$$\mathbf{V}_j(r, z, t) = \alpha\xi_j r\hat{\mathbf{e}}_\varphi + 2\xi_j\hat{\mathbf{e}}_z + f(t)\mathbf{B}_j(r, z), \tag{21}$$

where vector fields $\mathbf{B}_j(r, z)$ have the form (5) and satisfy the Beltrami equation (7). Formulae (20), (21) yield

$$\begin{aligned}
&\mathbf{V}_{MN}(r, z, t)\\
&\quad= \alpha\overline{\xi} r\hat{\mathbf{e}}_\varphi + 2\overline{\xi}\hat{\mathbf{e}}_z\\
&\qquad+ f(t)\Big[\sum_{n=1}^{M} a_{1n}\mathbf{B}_1(r, z + u_{1n})
\end{aligned}$$

$$+\sum_{n=1}^{M} a_{2n}\mathbf{B}_2(r, z+u_{2n})\Big]$$
$$+f(t)\sum_{k=1}^{N}\sum_{n=1}^{M}\Big[b_{kn}\frac{\partial^n\mathbf{B}_1(r, z+z_{kn})}{\partial z^n}$$
$$+c_{kn}\frac{\partial^n\mathbf{B}_2(r, z+\tilde{z}_{kn})}{\partial z^n}\Big], \tag{22}$$

where parameter $\overline{\xi} = \xi + \sum_{n=1}^{M}(a_{1n}\xi_1 + a_{2n}\xi_2)$. Here, vector fields $\partial^n\mathbf{B}_j(r, z+z_{kn})/\partial z^n$ (5) ($j = 1, 2$) correspond to the streamfunctions $\partial^n\psi_j(r, z+z_{kn})/\partial z^n$. The latter together with the streamfunctions $\psi_j(r, z)$ for $\mathbf{B}_j(r, z)$ evidently satisfy (6) because it is invariant under arbitrary differentiations $\partial^n/\partial z^n$ and translations $z \to z + z_{kn}$. Therefore, all vector fields $\partial^n\mathbf{B}_j(r, z+z_{kn})/\partial z^n$ and $\mathbf{B}_j(r, z+u_{jn})$ satisfy the Beltrami equation (7). Hence, vector field $\mathbf{V}_{MN}(r, z, t)$ (22) has the form

$$\mathbf{V}_{MN}(r, z, t) = \alpha\overline{\xi}r\hat{\mathbf{e}}_\varphi + 2\overline{\xi}\hat{\mathbf{e}}_z + f(t)\mathbf{B}_{MN}(r, z), \tag{23}$$

where vector field $\mathbf{B}_{MN}(r, z)$ is the linear combination of all steady Beltrami fields in (22), having the common factor $f(t)$. As the Beltrami equation (7) is linear, we get that vector field $\mathbf{B}_{MN}(r, z)$ also is a Beltrami field. Hence, vector fields $\mathbf{V}_{MN}(r, z, t)$ (20), (23) have the form (2) and therefore by Theorem 1 define exact solutions to the Navier–Stokes equations (1). The corresponding pressure $p_{MN}(r, z, t)$ is defined by the formula (3) with the new parameter $\overline{\xi} = \sum_{n=1}^{M}(a_{1n}\xi_1 + a_{2n}\xi_2)$. □

Remark 5: Theorem 2 proves that the space of exact solutions $\mathcal{L}_\alpha$ for a fixed parameter α and variable parameter ξ is linear with respect to the vector fields $\mathbf{V}(r, z, t)$ (2) and is nonlinear with respect to the pressure $p(r, z, t)$ (3).

Corollary 1: *The infinite-dimensional space $\mathcal{L}_\alpha$ of exact solutions* (2)–(3) *is invariant under the transformations:*

$$\mathbf{V}(r, z, t) \to F_{MN}(\mathbf{V}(r, z, t))$$
$$= \alpha\xi r\hat{\mathbf{e}}_\varphi + 2\xi\hat{\mathbf{e}}_z + \sum_{n=1}^{M} a_n\mathbf{V}(r, z+u_n, t)$$
$$+\sum_{k=1}^{N}\sum_{n=1}^{M} b_{kn}\frac{\partial^n\mathbf{V}(r, z+z_{kn}, t)}{\partial z^n}. \tag{24}$$

Here, a_n, u_n, b_{kn}, z_{kn} are arbitrary parameters.

Proof. Applying Theorem 2 for the case $\mathbf{V}_2(r, z, t) = \alpha\xi r\hat{\mathbf{e}}_\varphi + 2\xi\hat{\mathbf{e}}_z$, we get that transformations (24) are special cases of transforms (20). The transformations (24) commute with each other because the differentiations $\partial^n/\partial z^n$ commute with arbitrary translations $z \to z + u_k$. □

4 Backlund Transforms between the Axisymmetric Helmholtz Equation and the Linear Case of the Grad-Shafranov Equation

As known, the Helmholtz equation

$$\Delta F(\mathbf{x}) = -\alpha^2 F(\mathbf{x}) \tag{25}$$

for the z-axisymmetric functions $F(r, z)$ has the form

$$F_{rr} + \frac{1}{r}F_r + F_{zz} = -\alpha^2 F. \tag{26}$$

Consider two cases of the Grad–Shafranov equation [13, 14]

$$\psi_{rr} - \frac{1}{r}\psi_r + \psi_{zz} = -r^2\frac{\mathrm{d}P}{\mathrm{d}\psi} - G\frac{\mathrm{d}G}{\mathrm{d}\psi}, \tag{27}$$

corresponding to (*a*) $P(\psi) = 0$, $G(\psi) = \alpha\psi$ and (*b*) $P(\psi) = 0$, $G(\psi) = \sqrt{\beta^2 + \alpha^2\psi^2}$. For both cases, (27) becomes

$$\psi_{rr} - \frac{1}{r}\psi_r + \psi_{zz} = -\alpha^2\psi. \tag{28}$$

Equations (26) and (28) describe absolutely different physical phenomena. Therefore, the closeness in form of these equations is striking.

We introduce the new Backlund transforms between the axisymmetric Helmholtz equation (26) and the linear case (28) of the Grad–Shafranov equation, which coincides with (6). The Backlund transforms are used in Section 6 below.

Lemma 1: *(a) Backlund transform*

$$\psi(r, z) = r\frac{\partial F(r, z)}{\partial r} \tag{29}$$

maps any solution of (26) *into a solution to* (28).

(b) Backlund transform

$$F(t, z) = \frac{1}{r}\frac{\partial\psi(r, z)}{\partial r} \tag{30}$$

maps any solution of (28) *into a solution to* (26).

Proof. (*a*) Rewrite the Helmholtz equation (26) in the form $r^{-1}(rF_r)_r + F_{zz} = -\alpha^2 F$. Denoting here $rF_r = \psi$ and differentiating with respect to r, we find $r^{-1}\psi_{rr} - r^{-2}\psi_r + F_{rzz} = -\alpha^2 F_r$. Multiplying this equation with r and putting $rF_r = \psi$, we get (28).

(*b*) Represent the linear case (28) of the Grad–Shafranov equation in the form $r(r^{-1}\psi_r)_r + \psi_{zz} = -\alpha^2\psi$

and denote $r^{-1}\psi_r(r,z) = F(r,z)$. After differentiation with respect to r, we get $rF_{rr} + F_r + \psi_{rzz} = -\alpha^2\psi_r$. Multiplying with r^{-1} and putting $r^{-1}\psi_r = F$, we get (26). □

Remark 6: The composition of Backlund transforms (29) and (30) is

$$\tilde{F}(r,z) = F_{rr}(r,z) + r^{-1}F_r(r,z). \tag{31}$$

By Lemma 1, the mapping (31) is auto-Backlund transform of the axisymmetric Helmholtz equation (26); it has also the form $\tilde{F} = -F_{zz} - \alpha^2 F$.

Remark 7: The composition of Backlund transforms (30) and (29) is

$$\tilde{\psi}(r,z) = \psi_{rr}(r,z) - r^{-1}\psi_r(r,z). \tag{32}$$

The mapping (32) by Lemma 1 is the auto-Backlund transform of the linear case (28) of the Grad–Shafranov equation (27). The transform has also the form $\tilde{\psi} = -\psi_{zz} - \alpha^2\psi$.

5 Vortex Blobs and Vortex Rings

In view of (5), vector fields (2) have the form

$$\mathbf{V}_1(r,z,t) = -\frac{1}{r}\frac{\partial\psi_1}{\partial z}\hat{\mathbf{e}}_r + \frac{1}{r}\frac{\partial\psi_1}{\partial r}\hat{\mathbf{e}}_z + \frac{\alpha\psi_1}{r}\hat{\mathbf{e}}_\varphi, \tag{33}$$

where $\psi_1(r,z,t)$ is the time-dependent streamfunction:

$$\psi_1(r,z,t) = \xi r^2 + f(t)\psi(r,z). \tag{34}$$

Remark 8: The inner transforms (24) correspond to the following transformations of the streamfunctions $\psi_1(r,z,t)$:

$$\begin{aligned}\psi_1(r,z,t) &\to F_{MN}(\psi_1(r,z,t))\\ &= \xi r^2 + \sum_{n=1}^{M} a_n\psi_1(r,z+u_n)\\ &\quad + \sum_{k=1}^{N}\sum_{n=1}^{M} b_{kn}\frac{\partial^n\psi_1(r,z+z_{kn})}{\partial z^n}.\end{aligned} \tag{35}$$

Equation (33) implies that for any fixed moment of time t_0 the surface $\psi_1(r,z,t_0) = \text{const}$ (the angle $\varphi \in \mathbb{S}^1$ is arbitrary) is an invariant submanifold for the vorticity vector field $\nabla \times \mathbf{V}_1(r,z,t_0)$. This follows from formula (11): $\nabla\times\mathbf{V}_1 = \alpha\mathbf{V}_1 - \alpha^2\xi r\hat{\mathbf{e}}_\varphi$ and the z-axisymmetry of the flow.

As this surface $\psi_1(r,z,t_0) = \text{const}$ is z-axisymmetric, it is a disjoint union of either some spheres $\mathbb{S}^2$ or some tori $\mathbb{T}^2 = C_{\psi_1(t)}\times\mathbb{S}^1$ or some cylinders $\mathbb{C}^2 = R_{\psi_1(t)}\times\mathbb{S}^1$. Here, $C_{\psi_1(t)}$ and $R_{\psi_1(t)}$ are the level curves $\psi_1(r,z,t) = \text{const}$ in the poloidal plane (r,z) for a fixed time t. The curves $C_{\psi_1(t)} \subset (r,z)$ are closed, and the curves $R_{\psi_1(t)} \subset (r,z)$ are infinite. The circle $\mathbb{S}^1$ corresponds to the angular variable φ: $0 \le \varphi \le 2\pi$.

Assume that a surface $\psi_1(r,z,t_0) = C_1$ bounds a compact connected domain D_1. We call the domain D_1 maximal and denote it D_m if it is not contained in any bigger compact connected domain $\overline{D_m}$ bounded by a surface $\psi_1(r,z,t_0) = \overline{C_1}$. If such a maximal domain D_m intersects the axis of symmetry $r = 0$, then topologically it is a z-axisymmetric ball $\mathbb{B}^3_m$, which we call a vortex blob because it is invariant with respect to the vorticity field $\nabla \times \mathbf{V}_1(r,z,t_0)$.

Remark 9: Suppose that function $\psi(r,\ z)$ in (34) is obtained by transform (29). Then on the axis of symmetry $r = 0$, we have $\psi_1(0,z,t) = 0$. As the vortex blobs D_m intersect the axis $r = 0$, the same is true for their boundaries defined by equation $\psi_1(r,z,t) = C_m$. Putting here $r = 0$, we get $C_m = 0$. Hence, the boundaries of the vortex blobs satisfy the equation

$$\psi_1(r,z,t) = 0. \tag{36}$$

Equation (36) can define several connected components; see exact solutions in Section 6 and 8.

If $C_m \neq 0$, then the corresponding maximal compact connected domain D_m bounded by the surface $\psi_1(r,z,t_0) = C_m \neq 0$ does not intersect the axis of symmetry $r = 0$ because $\psi_1(0,z,t_0) = 0$. Therefore, the domain D_m for $C_m \neq 0$ topologically is a 3-dimensional z-axisymmetric ring $\mathbb{B}^2_m(t_0)\times\mathbb{S}^1$, where $\mathbb{B}^2_m(t_0) \subset (r,z)$ topologically is equivalent to a 2-dimensional ball in the poloidal plane (r,z). The boundary of the ring $\mathbb{B}^2_m(t_0)\times\mathbb{S}^1$ is a torus $\mathbb{T}^2 = C_{\psi_1(t_0)}\times\mathbb{S}^1$ where $C_{\psi_1(t_0)} = \partial\mathbb{B}^2_m(t_0)$ is a closed level curve $\psi_1(r,z,t_0) = C_m \neq 0$, $\varphi = 0$. As the ring $\mathbb{B}^2_m(t_0)\times\mathbb{S}^1$ is invariant with respect to the vorticity field $\nabla\times\mathbf{V}_1(r,z,t_0)$, we call it a vortex ring. In view of (11), the vortex blobs and vortex rings are invariant also with respect to the velocity field $\mathbf{V}_1(r,z,t_0)$.

As known, for an ideal incompressible fluid, the vorticity field $\nabla \times \mathbf{V}(\mathbf{x},t)$ is frozen into the fluid flow. Therefore, for the inviscid fluid ($\nu = 0$), the vortex blobs and vortex rings are transported with the fluid flow. For a viscous fluid with $\nu(t) \neq 0$, the vortex blobs and vortex rings are not frozen into the viscous fluid flow and undergo a more sophisticated dynamics and can collapse and disappear at some moments of time t.

Both vortex blobs and vortex rings are equivalently represented by their intersections with the poloidal plane

(r, z), $\varphi = 0$. Below we study dynamics in time t of the poloidal sections of the vortex blobs and vortex rings for the concrete exact solutions derived in Section 6.

6 Bifurcations in Exact Solutions to the Navier–Stokes Equations

I. The Helmholtz equation (25) for the spherical functions $F(R)$, $R = \sqrt{r^2 + z^2}$, has the form $F_{RR} + 2F_R/R = -\alpha^2 F$. This equation has an important exact solution $F(R) = \sin(\alpha R)/R$.[1] The solution evidently is z-axisymmetric and therefore satisfies (26). Applying the Backlund transform (29), we get that function

$$\psi(r,z) = -\frac{r}{\alpha^3}\frac{\partial F(r,z)}{\partial r} = -r^2 G_2(\alpha R)$$
$$= -\frac{r^2}{\alpha^2 R^2}\left[\cos(\alpha R) - \frac{\sin(\alpha R)}{\alpha R}\right] \qquad (37)$$

satisfies (28) [or (6)]. Therefore, the corresponding z-axisymmetric vector field $\mathbf{B}(r, z)$ (5) by Theorem 1 satisfies the Beltrami equation (7). Function $G_2(u)$ in (37), $G_2(u) = u^{-2}(\cos u - u^{-1}\sin u)$, is connected with the Bessel function $J_{3/2}(u)$ of order 3/2 by the relation

$$G_2(u) = -\frac{\sqrt{\pi/2}}{u^{3/2}}J_{3/2}(u).$$

Remark 10: In another form, Beltrami field $\mathbf{B}(r, z)$ [(5) and (37)] was first derived in 1899 in the pioneer article by W.M. Hicks [16] that is the historical precursor of many works on fluid and plasma equilibria.[2] The Beltrami field $\mathbf{B}(r, z)$ (5), (37) was rediscovered in the theory of plasma equilibria in terms of Bessel functions $J_{3/2}(u)$ [19] by Chandrasekhar [20] and Woltjer [21] as a model of axisymmetric plasma equilibria and is called the spheromak field. The term "spheromak" was first introduced in [22]; see review [23]. Moduli spaces of vortex knots for the spheromak Beltrami field in different invariant domains were presented in [24] and for another Beltrami field in [25].

II. We will use in this article the following functions $G_n(u)$ connected with the Bessel functions $J_{n-1/2}(u)$:

$$G_0(u) = -\cos u,$$

$$G_1(u) = \frac{\mathrm{d}}{u\mathrm{d}u}G_0(u) = \frac{\sin u}{u} = \frac{\sqrt{\pi/2}}{u^{1/2}}J_{1/2}(u),$$

$$G_2(u) = \frac{\mathrm{d}}{u\mathrm{d}u}G_1(u) = \frac{1}{u^2}\left[\cos u - \frac{\sin u}{u}\right]$$
$$= -\frac{\sqrt{\pi/2}}{u^{3/2}}J_{3/2}(u),$$

$$G_3(u) = \frac{\mathrm{d}}{u\mathrm{d}u}G_2(u) = \frac{1}{u^4}\left[(3-u^2)\frac{\sin u}{u} - 3\cos u\right]$$
$$= \frac{\sqrt{\pi/2}}{u^{5/2}}J_{5/2}(u).$$

$$G_4(u) = \frac{\mathrm{d}}{u\mathrm{d}u}G_3(u)$$
$$= \frac{1}{u^6}\left[(6u^2-15)\frac{\sin u}{u} - (u^2-15)\cos u\right]$$
$$= -\frac{\sqrt{\pi/2}}{u^{7/2}}J_{7/2}(u). \qquad (38)$$

All functions $G_n(u)$ are analytic everywhere and have the nonzero values at $u = 0$:

$$G_1(0) = 1, \quad G_2(0) = -1/3,$$
$$G_3(0) = 1/15, \quad G_4(0) = -1/105. \qquad (39)$$

The plot of function $y_1(u) = G_2(u)$ is shown in Figure 1. The range of function $G_2(u)$ is the segment $I^* = (-1/3, \xi_1 \approx 0.02872)$.

Functions $G_n(u)$ (38) are even and satisfy the easily verifiable identities

$$G_0(u) + G_1(u) + u^2 G_2(u) = 0,$$
$$G_1(u) + 3G_2(u) + u^2 G_3(u) = 0. \qquad (40)$$

The general identity

$$G_n(u) + (2n+1)G_{n+1}(u) + u^2 G_{n+2}(u) = 0, \qquad (41)$$

for $G_{k+1}(u) = u^{-1}\mathrm{d}G_k(u)/\mathrm{d}u$ follows from identities (40) by induction.

III. Vector field $\mathbf{V}_1(r, z, t)$ (33) with the streamfunction

$$\psi_1(r,z,t) = r^2\left[\xi - f(t)G_2(\alpha R)\right] \qquad (42)$$

1 Applications of the exact solution $\sin(\alpha R)/R$ to the atomic bomb physics were analysed by W. Heisenberg, see pp. 193 and 194 of his lecture [15].

2 The author has found in the literature another article by Hicks [17] that is the abstract of [16] published separately in 1898. Therefore, the two articles [16, 17] should be read together. Their analysis from a comprehensive point of view is shown in Section 9 "Comments on Hicks' Papers" of our work [18].

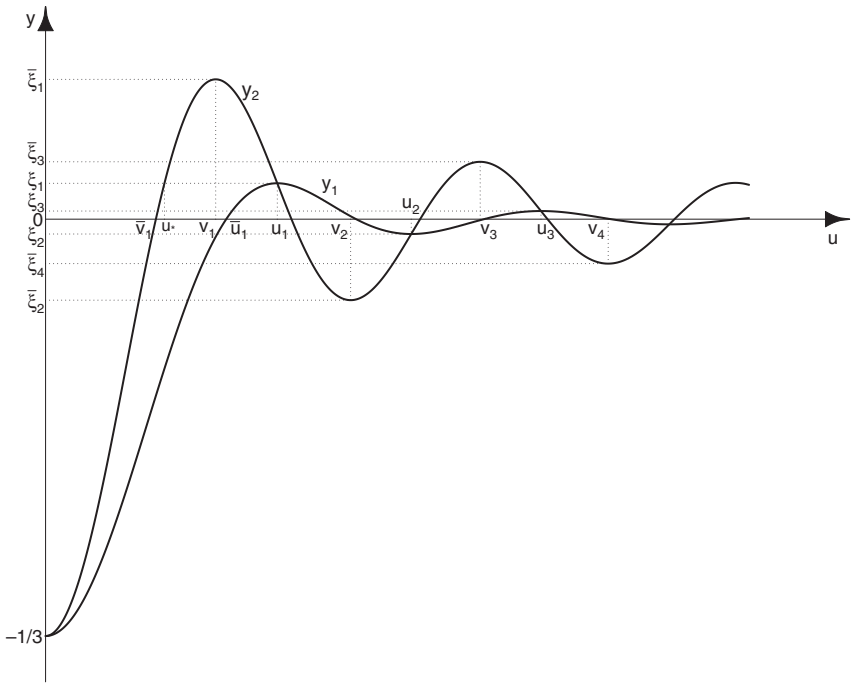

Figure 1: Plots of functions $y_1(u) = G_2(u)$ and $y_2(u) = -(G_1(u) + G_2(u))/2$.

has the form

$$\begin{aligned}\mathbf{V}_1(r,z,t) &= \alpha^2 rzf(t)G_3(\alpha R)\hat{\mathbf{e}}_r \\ &\quad + \Big[2\xi - f(t)(2G_2(\alpha R) + \alpha^2 r^2 G_3(\alpha R))\Big]\hat{\mathbf{e}}_z \\ &\quad + \alpha r\big[\xi - f(t)G_2(\alpha R)\big]\hat{\mathbf{e}}_\varphi, \end{aligned} \tag{43}$$

where $f(t)$ is the function (4). This vector field together with the pressure $p(r,z,t)$ (3) defined by the formula

$$\begin{aligned}p(r,z,t) = \rho\Big[&C + \Psi(r,z,t) + \alpha^2 r^2 \xi\big[\xi - f(t)G_2(\alpha R)\big] \\ &- \frac{1}{2}|\mathbf{V}_1(r,z,t)|^2\Big]\end{aligned}$$

is the new exact solution to the Navier–Stokes equations (1).

Remark 11: For the vanishing viscosity $\nu(t) = 0$, function $f(t)$ (4) equals 1. Fluid flows (43) for $f(t) = \text{const}$ and arbitrary parameters α, ξ are equivalent to the steady solutions to Euler equations for the ideal incompressible fluid studied in [26].

Remark 12: For exact solutions (42), (43), we find $\psi_1(0,z,t) = 0$ for $r = 0$. Hence, the boundary of a vortex blob is defined by equation $\psi_1(r,z,t) = 0$ (36); see Remark 9 above. Therefore, on the boundary, we have $\xi = f(t)G_2(\alpha R)$. Hence, the vortex blob is a ball $\mathbb{B}^3_{a_k}$ of radius a_k defined by the equation

$$G_2(\alpha a_k) = \xi/f(t) = \xi \exp\left(\alpha^2 \int_0^t \nu(\tau)\mathrm{d}\tau\right) \tag{44}$$

and its boundary is the sphere $\mathbb{S}^2_{a_k}$ of radius $R = a_k$.

IV. Function $G_2(u) \to 0$ when $u \to \infty$ and has infinitely many oscillations, see its formula in (38). Therefore, from Figure 1, it becomes evident that equation $G_2(u) = \xi/f(t)$ (44) for $\xi \neq 0$, $\xi/f(t) \in I^* = (-1/3, \xi_1 \approx 0.02872)$, has a finite number $N(t)$ of roots and $N(t) \to \infty$ when $\xi/f(t) \to 0$. That means the vector field $\mathbf{V}_1(r,z,t)$ in the whole space $\mathbb{R}^3$ can have for $\xi \neq 0$ a finite number $N(t)$ of invariant spheroids $\mathbb{B}^3_{a_i}$, and it has infinitely many invariant spheroids when $\xi = 0$.

The velocity field $\mathbf{V}_1(r,z,t)$ (43) does not have any invariant spheroids $\mathbb{B}^3_c$ ($R \leq c$) for time t satisfying condition $\xi/f(t) \notin I^*$ because for this case (44) has no solutions; see Figure 1.

Dynamical system defined by the vector field $\mathbf{V}_1(r,z,t)$ (33), (43) has the form

$$\dot{r} = \alpha^2 rzf(t)G_3(\alpha R),$$

$$\dot{z} = 2\xi - f(t)\Big[2G_2(\alpha R) + \alpha^2 r^2 G_3(\alpha R)\Big], \tag{45}$$

$$\dot{\varphi} = \alpha[(\xi - f(t)G_2(\alpha R)]. \tag{46}$$

Dynamics of fluid vanishes on the spheres $R = R_k$, where $G_3(\alpha R_k) = 0$ at the moments of time t_k defined by equation $f(t_k) = \xi/G_2(\alpha R_k)$.

Equilibrium points (at a fixed time t) of dynamical system (45) are defined by equations $z = 0$ and

$$[2G_2(u) + u^2 G_3(u)]/2 = \xi/f(t), \tag{47}$$

where $u = \alpha R$. The second identity (40) yields $2G_2(u) + u^2 G_3(u) = -G_1(u) - G_2(u)$. Therefore, (47) takes the form

$$y_2(u) = -\frac{G_1(u) + G_2(u)}{2} = -\frac{1}{2}\left[\frac{\sin u}{u} + \frac{1}{u^2}\left(\cos u - \frac{\sin u}{u}\right)\right] = \xi/f(t). \tag{48}$$

The plot of function $y_2(u)$ (48) is shown in Figure 1. The range of function $y_2(u)$ is the segment $(-1/3, \overline{\xi}_1 \approx 0.11182)$. Thus, oscillations of function $y_2(u)$ are greater than those of function $y_1(u)$; see Figure 1. Function $y_2(u) \to 0$ when $u \to \infty$. Therefore, the number $M(t)$ of roots of (48) is finite for all t and $M(t) \to \infty$ when $\xi/f(t) \to 0$.

The stream surfaces $\psi_1(r, z, t) = \text{const}$ for solutions (42), (43) are up-down symmetric and have different structure for $\xi > 0$ and $\xi < 0$. The poloidal contours of the stream surfaces for $\xi > 0$ are shown (for $\alpha = 1$) in Figures 2–11 for a sequence of increasing moments of time t: $-\infty, t_1 < t_2 < \cdots < t_8, \infty$. In Figures 12–19, we show the poloidal contours of the stream surfaces for $\xi < 0$, $\alpha = 1$ for a sequence of increasing moments of time t^*: $-\infty, t_1^* < t_2^* < \cdots < t_6^*, \infty$. The arrows in Figures 2–19 show the direction of the dynamics defined by system (45).

For the solutions (42), (43), all vortex blobs are the balls bounded by certain spheres $R = a_k$ (44); they are shown in blue. The roots $u_k = \alpha R_k$ of (48) for a given time

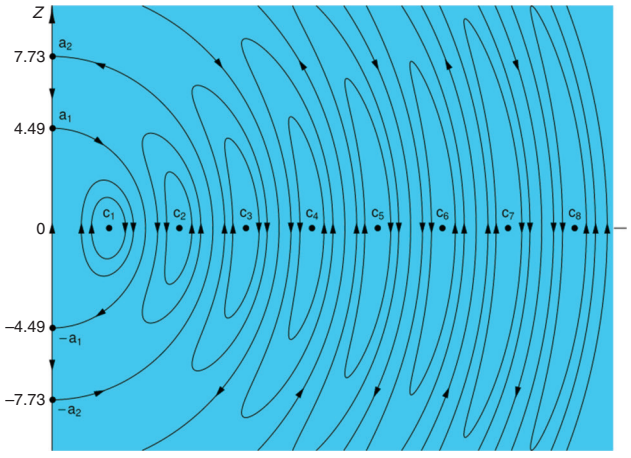

Figure 2: Time $t = -\infty$, $\xi > 0$.

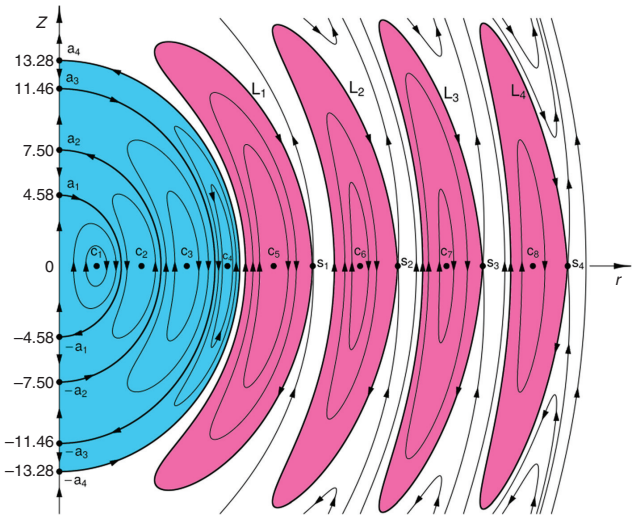

Figure 3: Time t_1: $f(t_1) = \xi/0.004$.

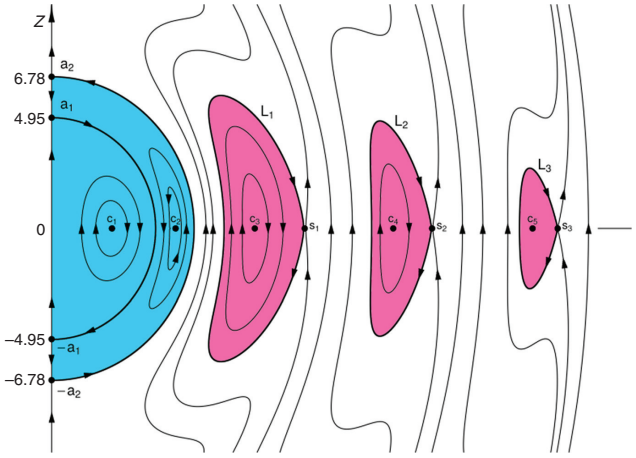

Figure 4: Time t_2: $f(t_2) = \xi/0.0176$.

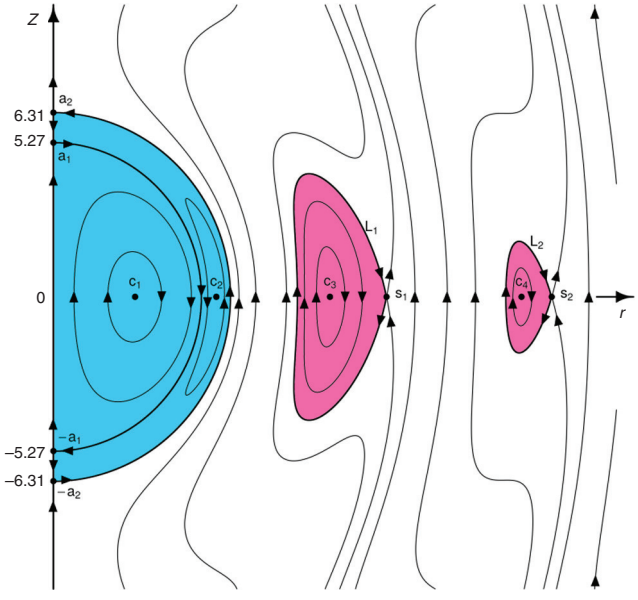

Figure 5: Time t_3: $f(t_3) = \xi/0.025$.

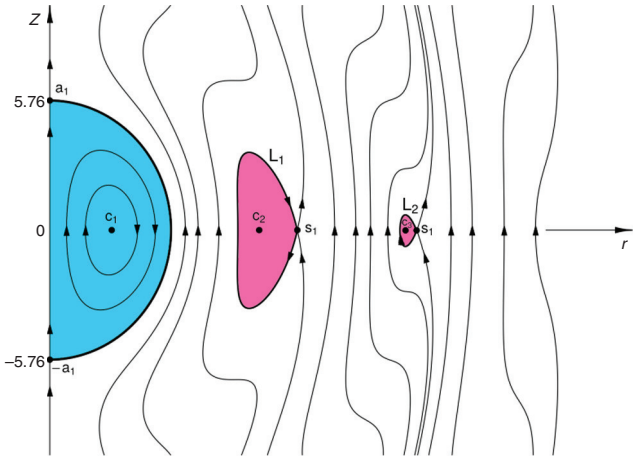

Figure 6: Time t_4: $f(t_4) = \xi/0.02872$.

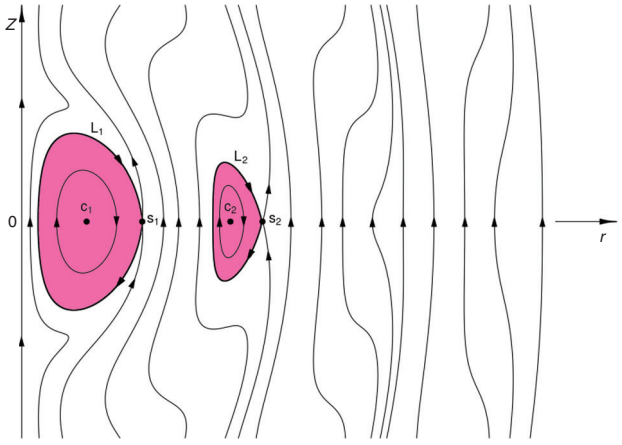

Figure 7: Time t_5: $f(t_5) = \xi/0.0326$.

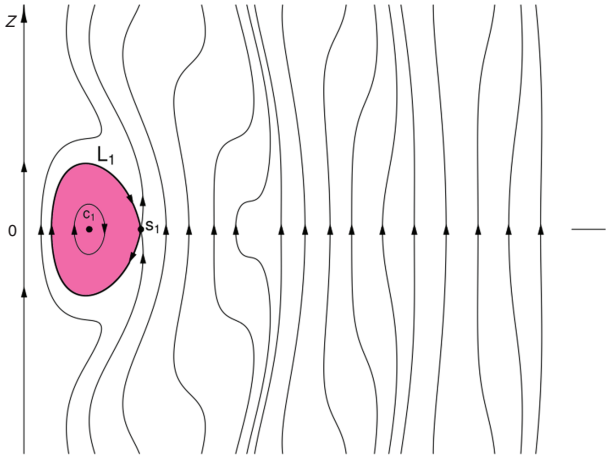

Figure 8: Time t_6: $f(t_6) = \xi/0.0461$.

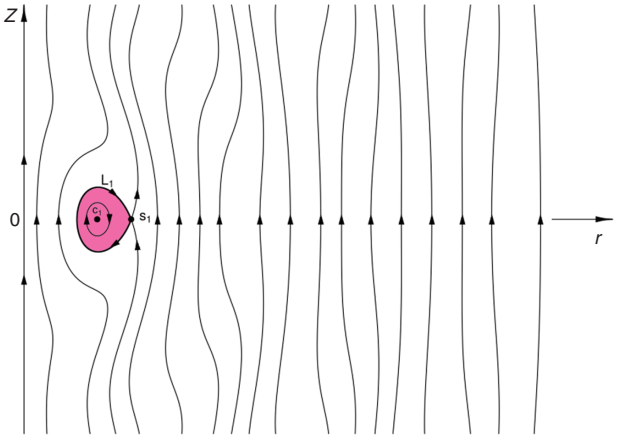

Figure 9: Time t_7: $f(t_7) = \xi/0.0788$.

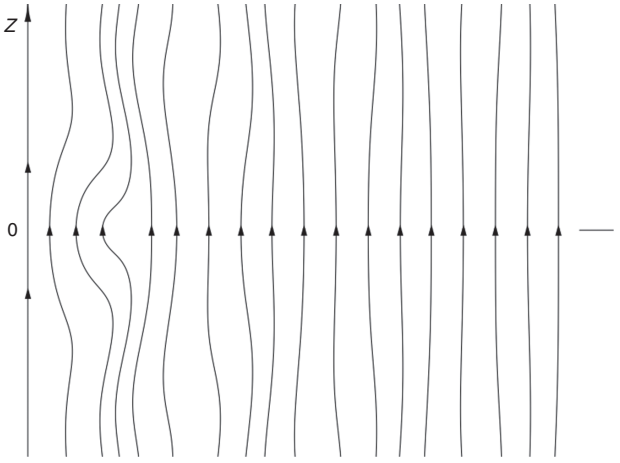

Figure 10: Time t_8: $f(t_8) = \xi/0.132$.

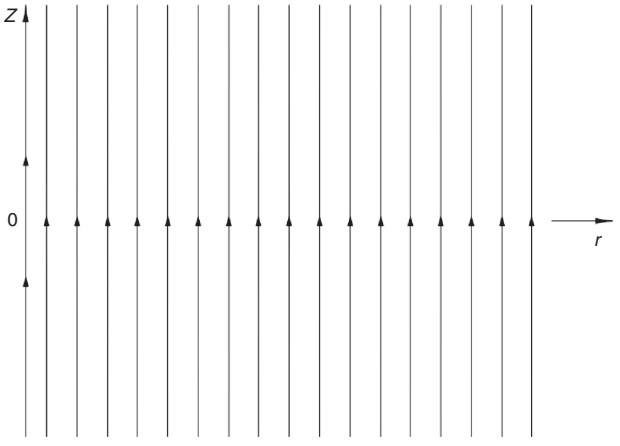

Figure 11: Time $t = +\infty$.

t that are greater than all roots αa_j of (44) define equilibria ($r = R_k, z = 0$), which belong to the vortex rings that are shown in Figures 2–9 in pink. The roots $u_k = \alpha R_k$ (48) are extreme of function $\psi_1(r, z, t)$ (42); they are denoted in Figures 2–19 as c_j, a_i, and s_k. Points c_j are stable maxima or minima of function $\psi_1(r, z, t)$; points a_i and s_k are unstable saddles. The interiors of each vortex ball and vortex ring are filled with invariant tori $\mathbb{T}^2 = C^1_{\psi_1(t)} \times \mathbb{S}^1$ of dynamical system (45) to (46), where $C^1_{\psi_1(t)} \subset (r, z)$ is a

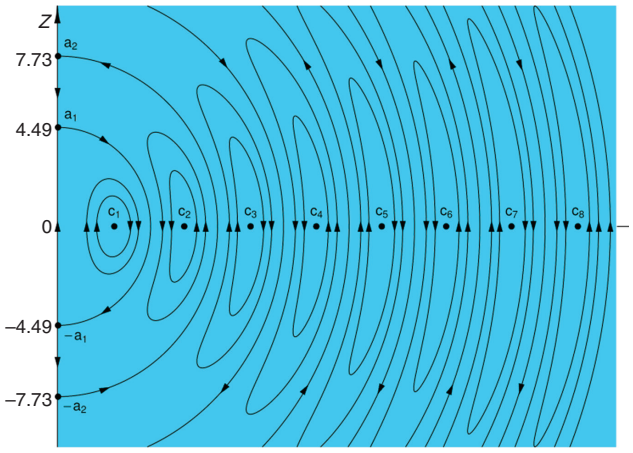

Figure 12: Time $t = -\infty$, $\xi < 0$.

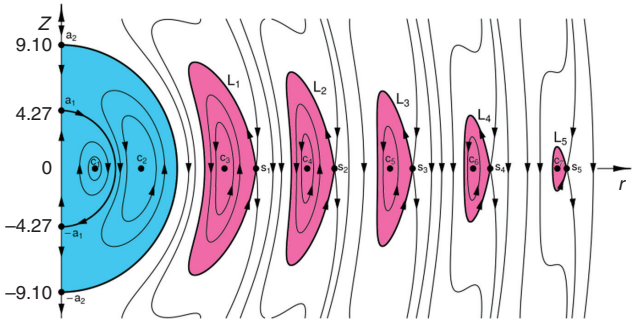

Figure 13: Time t_1^*: $f(t_1^*) = |\xi|/0.0119$.

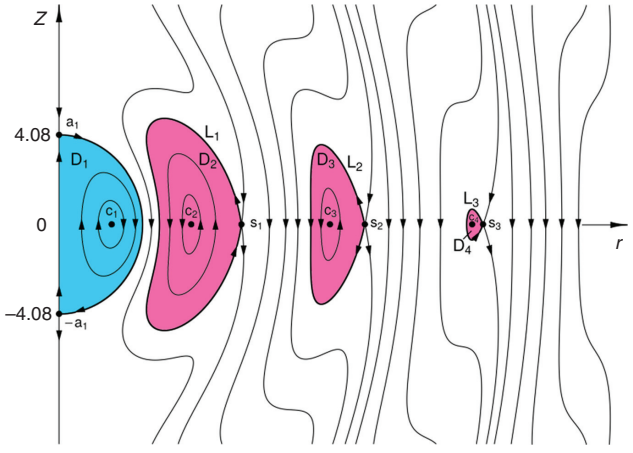

Figure 14: Time $t = t_2^*$: $f(t_2^*) = |\xi|/0.0237$.

closed curve defined by equation $\psi_1(r, z, t) = \text{const}$ (for the given moment of time t).

When $\xi/f(t)$ satisfies the inequalities

$$\xi_1 \approx 0.02872 < \xi/f(t) < \overline{\xi}_1 \approx 0.11182, \quad \xi > 0, \quad (49)$$

the vector field $\mathbf{V}_1(r, z, t)$ (43) has finitely many vortex rings and no vortex balls; see Figures 7–9. Figures 2–19 illustrate dynamics of vortex balls and vortex rings. It is

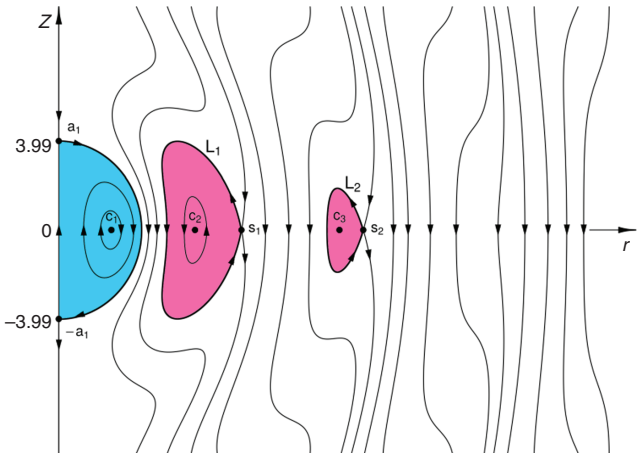

Figure 15: Time t_3^*: $f(t_3^*) = |\xi|/0.03$.

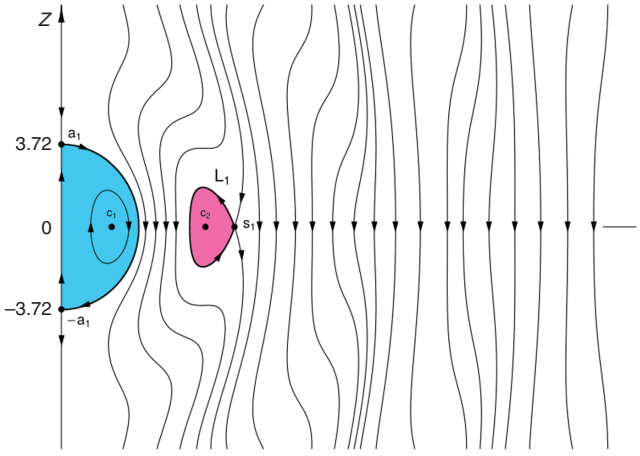

Figure 16: Time t_4^*: $f(t_4^*) = |\xi|/0.0501$.

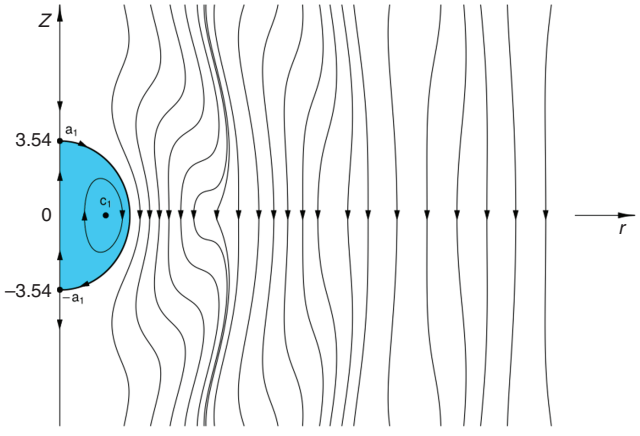

Figure 17: Time t_5^*: $f(t_5^*) = |\xi|/0.0652$.

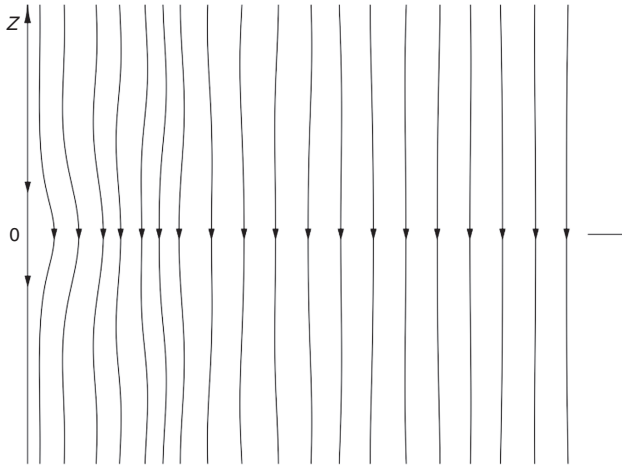

Figure 18: t_6^*: $f(t_6^*) = |\xi|/0.36$.

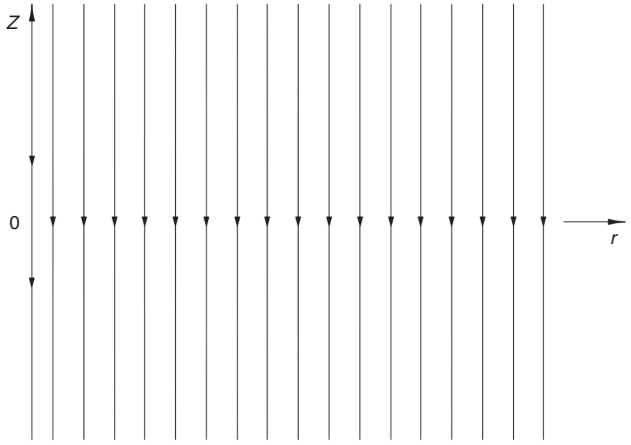

Figure 19: Time $t = +\infty$.

evident from these Figures that vortex balls and vortex rings as $t \to \infty$ collapse and disappear.

V. Using (11), we find the corresponding to (43) vorticity field

$$\begin{aligned}\nabla \times \mathbf{V}_1(r,z,t) &= \alpha^3 rzf(t)G_3(\alpha R)\hat{\mathbf{e}}_r \\ &+ \alpha\Big[2\xi - f(t)(2G_2(\alpha R) + \alpha^2 r^2 G_3(\alpha R))\Big]\hat{\mathbf{e}}_z \\ &- \alpha^2 rf(t)G_2(\alpha R)\hat{\mathbf{e}}_\varphi. \end{aligned} \tag{50}$$

In the Cartesian coordinates (x, y, z), the new solution $\mathbf{V}_1(r, z, t)$ has the form

$$\begin{aligned}\mathbf{V}_1(\mathbf{x},t) = {} & [-\alpha\xi y + f(t)(\alpha y G_2 + \alpha^2 xzG_3)]\hat{\mathbf{e}}_x \\ & + [\alpha\xi x + f(t)(-\alpha x G_2 + \alpha^2 yzG_3)]\hat{\mathbf{e}}_y \\ & + [2\xi + f(t)(G_1 + G_2 + \alpha^2 z^2 G_3)]\hat{\mathbf{e}}_z, \end{aligned} \tag{51}$$

where we substituted $2G_2 + \alpha^2 r^2 G_3 = -(G_1 + G_2 + \alpha^2 z^2 G_3)$ [applying the second identity (40)]. Everywhere $G_n = G_n(\alpha R)$.

Remark 13: The exact solutions (43), (51) for $\xi > 0$ and for $\xi < 0$ have the following important distinctions that follow from (44), (48):

(*a*) If the flow for $\xi > 0$ at a time t has a vortex blob, then it does have at least one vortex ring; see Figures 3–6. For $\xi > 0$, there is interval of time t satisfying inequalities (49) when the flow has vortex rings but does not have a vortex blob; see Figures 7–9.

(*b*) For $\xi < 0$, there is interval of time t satisfying inequalities

$$-1/3 < \xi/f(t) < \overline{\xi}_2 \approx -0.0648, \quad \xi < 0,$$

when the flow has a vortex blob but does not have any vortex rings; see Figure 17. However, if for $\xi < 0$ the flow (43), (51) has a vortex ring, then it necessarily has a vortex blob; see Figures 13–16.

7 Discontinuous Volume Function $V_m(t)$

I. At any fixed time $t = t_0$, the fluid velocity field $\mathbf{V}_1(r, z, t_0)$ (43) and vorticity field $\nabla \times \mathbf{V}_1(r, z, t_0)$ (50) are tangent to the surfaces of constant level of the streamfunction $\psi_1(r, z, t_0)$ (42).

The zero level of function (42) at a fixed time t is the union of several spheres $\mathbb{S}^2_{a_i(t)}$ of radii $a_i(t)$ obeying equation $G_2(\alpha a_i(t)) = \xi/f(t)$ or

$$G_2(\alpha a_i(t)) = \xi \exp\left(\alpha^2 \int_0^t \nu(\tau)\mathrm{d}\tau\right). \tag{52}$$

Vector fields $\mathbf{V}_1(r, z, t)$ (43) and $\nabla \times \mathbf{V}_1(r, z, t)$ (50) on each sphere $\mathbb{S}^2_{a_i(t)}$ have the form

$$\overline{\mathbf{V}}_1(r,z,t) = \alpha^2 rf(t)G_3(\alpha a_i(t))\big[z\hat{\mathbf{e}}_r - r\hat{\mathbf{e}}_z\big], \tag{53}$$

$$\begin{aligned}\overline{\nabla \times \mathbf{V}}_1(r,z,t) = {} & \alpha^3 rf(t)G_3(\alpha a_i(t))\big[z\hat{\mathbf{e}}_r - r\hat{\mathbf{e}}_z\big] \\ & - \alpha^2 r\xi\hat{\mathbf{e}}_\varphi. \end{aligned} \tag{54}$$

It is evident from (53) to (54) that the spheres $\mathbb{S}^2_{a_i(t)}$ are invariant submanifolds for the flows $\mathbf{V}_1(r, z, t)$ and $\nabla \times \mathbf{V}_1(r, z, t)$. Therefore, the balls $\mathbb{B}^3_{a_i(t)}$ bounded by the spheres $\mathbb{S}^2_{a_i(t)}$ also are invariant under the vorticity field $\nabla \times \mathbf{V}_1(r, z, t)$. Therefore, we call the ball $\mathbb{B}^3_{a_m(t)}$ of the maximal radius $a_m(t)$ a vortex blob.

From Figure 1, it is evident that for $\xi > 0$ the number of solutions $a_i(t)$ to (52) is even, say equal to $2N(t)$. Therefore, inside the vortex blob $\mathbb{B}^3_{a_m(t)}$, there are $2N(t)-1$ invariant balls

$$\mathbb{B}^3_{a_1(t)} \subset \mathbb{B}^3_{a_2(t)} \subset \cdots \mathbb{B}^3_{a_{2N(t)-1}(t)} \subset \mathbb{B}^3_{a_m(t)}. \tag{55}$$

For $\xi < 0$, the number of solutions $a_i(t)$ to (52) is odd, say equal to $2N(t)+1$. Hence, inside the vortex blob $\mathbb{B}^3_{a_m(t)}$, there are $2N(t)$ invariant balls

$$\mathbb{B}^3_{a_1(t)} \subset \mathbb{B}^3_{a_2(t)} \subset \cdots \mathbb{B}^3_{a_{2N(t)}(t)} \subset \mathbb{B}^3_{a_m(t)}. \tag{56}$$

At $t \to -\infty$, we have $\exp\left(\alpha^2 \int_0^t \nu(\tau)\mathrm{d}\tau\right) \to 0$. Hence, formula (52) and Figure 1 yield $N(t) \to \infty$ when $t \to -\infty$.
II. The fluid flow (53) becomes identically zero on the spheres $\mathbb{S}^2_{a_\ell(t)}$ defined by equation $G_3(\alpha a_\ell(t)) = 0$. As $G_3(u) = u^{-1}\mathrm{d}G_2(u)/\mathrm{d}u$, the equation $G_3(u_\ell) = 0$ means that the point $u_\ell = \alpha a_\ell(t)$ is a point of either local maximum or local minimum of function $y_1(u) = G_2(u)$; see Figure 1. In view of (38), equation $G_3(u) = 0$ is equivalent to equation

$$\tan u = \frac{3u}{3-u^2}. \tag{57}$$

The first eight roots u_ℓ of (57) are

$$u_1 \approx 5.7635, \quad u_2 \approx 9.0950,$$
$$u_3 \approx 12.3229, \quad u_4 \approx 15.5146,$$
$$u_5 \approx 18.6890, \quad u_6 \approx 21.8539,$$
$$u_7 \approx 25.0128, \quad u_8 \approx 28.1678.$$

The corresponding values $\xi_\ell = G_2(u_\ell)$ are as follows:

$$\xi_1 = G_2(u_1) \approx 0.02872, \quad \xi_2 \approx -0.0119,$$
$$\xi_3 \approx 0.0065, \quad \xi_4 \approx -0.0041, \quad \xi_5 \approx 0.0029,$$
$$\xi_6 \approx -0.0021, \quad \xi_7 \approx 0.0016, \quad \xi_8 \approx -0.0013. \tag{58}$$

The positive values $\xi_\ell > 0$ are local maxima of function $G_2(u)$; the negative values $\xi_\ell < 0$ are local minima; see Figure 1.

The vortex blob $\mathbb{B}^3_{a_m(t)}$ and invariant spheres $\mathbb{S}^2_{a_i(t)}$ exist if (52) has some roots $a_i(t)$. This is possible only if $\xi \exp\left(\alpha^2 \int_0^t \nu(\tau)\mathrm{d}\tau\right)$ belongs to the range of function $G_2(u)$. The plot of function $y_1(u) = G_2(u)$ in Figure 1 shows that the range of function $G_2(u)$ is the segment $[-1/3, \xi_1 \approx 0.02872]$. Here, ξ_1 is the maximal value of function $y_1(u) = G_2(u)$. It is attained at the point u_1 satisfying equation $G_3(u) = u^{-1}\mathrm{d}G_2(u)/\mathrm{d}u = 0$. The first root of equation $G_3(u) = 0$ (57) is $u_1 \approx 5.7635$. Hence, we calculate $G_2(u_1) = \xi_1 \approx 0.02872$.
III. Consider (52) for $a_m(t)$ and differentiate it with respect to time t. Using equation $\mathrm{d}G_2(u)/\mathrm{d}u = uG_3(u)$ (38), we find

$$\alpha^2 a_m(t) G_3(\alpha a_m(t)) \frac{\mathrm{d}a_m(t)}{\mathrm{d}t}$$
$$= \alpha^2 \nu(t) \xi \exp\left(\alpha^2 \int_0^t \nu(\tau)\mathrm{d}\tau\right)$$
$$= \alpha^2 \nu(t) G_2(\alpha a_m(t)).$$

Hence, we get

$$\frac{\mathrm{d}a_m(t)}{\mathrm{d}t} = \nu(t) \frac{G_2(\alpha a_m(t))}{a_m(t) G_3(\alpha a_m(t))}. \tag{59}$$

The volume $V_m(t)$ of the vortex blob $\mathbb{B}^3_{a_m(t)}$ is $4\pi a_m^3(t)/3$. Hence, from (59), we derive

$$\frac{\mathrm{d}V_m(t)}{\mathrm{d}t} = 4\pi\nu(t) \frac{a_m(t) G_2(\alpha a_m(t))}{G_3(\alpha a_m(t))}. \tag{60}$$

Equation (60) shows that the speed of the change of the vortex blob volume $V_m(t)$ is proportional to the kinematic viscosity $\nu(t)$ of the fluid.
IV. For $\xi > 0$, (52) yields that function $G_2(\alpha a_m(t)) > 0$. As $u_m(t) = \alpha a_m(t)$ is the maximal root of (52), we see from Figure 1 that $\mathrm{d}G_2(u)/\mathrm{d}u < 0$ at $u = u_m(t)$. Hence, $G_3(u_m(t)) = u_m^{-1}(t)\mathrm{d}G_2(u_m(t))/\mathrm{d}u < 0$. Therefore, from (60), we get $\mathrm{d}V_m(t)/\mathrm{d}t < 0$. Hence, function $V_m(t)$ is monotonously decreasing.

Equation (60) shows that derivative $\mathrm{d}V_m(t)/\mathrm{d}t = -\infty$ at the moment of time $t = t_k$ when $G_3(\alpha a_m(t_k)) = 0$. Function $G_2(u)$ has local maximum at $u = u_k = \alpha a_m(t_k)$, and for $t = t_k + \varepsilon$, there is no invariant sphere of radius close to $a_m(t_k)$ because the two neighbouring spheres $\mathbb{B}^3_{a_{2N(t)-1}}$ and $\mathbb{B}^3_{a_m(t)}$ coincide at $t = t_k$ and then disappear. Therefore, the next ball $\mathbb{B}^3_{a_{2N(t)-2}}$ in the nested sequence (55) becomes maximal. Hence, the radius $a_m(t_k)$ of the vortex blob jumps down to the value $a_{2N(t)-2}(t_k)$ at the moment t_k. The volume $V_m(t) = 4\pi a_m^3(t)/3$ jumps down correspondently. The jumps occur at the moments of time t_k when function $G_2(\alpha a_m(t))$ takes the positive values ξ_k (58). From (52), we get equation for the corresponding times t_k:

$$\int_0^{t_k} \nu(\tau)\mathrm{d}\tau = \alpha^{-2} \log(\xi_k/\xi), \tag{61}$$

where $\xi_k = G_2(u_k) > 0$, and u_k satisfies equation $G_3(u_k) = 0$, $a_m(t_k) = u_k/\alpha$.

For $\xi > 0$, (52) yields that the maximal time $t = t_m$ when the fluid flow $\mathbf{V}_1(r, z, t)$ (43) has a vortex blob $\mathbb{B}^3_{a_m(t_m)}$ is defined by the condition $G_2(\alpha a_m(t_m)) = \xi_1 \approx 0.02872$. At this moment, $\alpha a_m(t_m) = u_1 \approx 5.7635$. Hence, we get from (52) the equation for the time t_m:

$$\int_0^{t_m} \nu(\tau)\mathrm{d}\tau = \alpha^{-2}\log(\xi_1/\xi)$$

$$\approx \alpha^{-2}\log(0.02872/\xi). \tag{62}$$

The last vortex blob (ball) $\mathbb{B}^3_{a_m(t_m)}$ has the minimal possible radius $a_m(t_m) = u_1/\alpha \approx 5.7635/\alpha$. Equation (53) yields that the fluid velocity $\mathbf{V}_1(r, z, t_m)$ is identically zero on the boundary sphere $\mathbb{S}^2_{a_m(t_m)}$. For all times $t > t_m$, the fluid flow $\mathbf{V}_1(r, z, t)$ (43) does not have any vortex blob.

The plot of the monotonously decreasing discontinuous function $V_m(t)$ is shown in Figure 20.

V. Equation (52) for $\xi < 0$ yields that function $G_2(\alpha a_m(t)) < 0$. The range of negative values of $G_2(u)$ is the segment $[-1/3, 0]$. As $u_m(t) = \alpha a_m(t)$ is the maximal root of (52), we see from Figure 1 that $\mathrm{d}G_2(u)/\mathrm{d}u > 0$ at $u = u_m(t)$. Hence, $G_3(u_m(t)) = u_m^{-1}(t)\mathrm{d}G_2(u_m(t))/\mathrm{d}u > 0$. Therefore, from (60), we get $\mathrm{d}V_m(t)/\mathrm{d}t < 0$. Hence, function $V_m(t)$ is monotonously decreasing.

Equation (60) shows that derivative $\mathrm{d}V_m(t)/\mathrm{d}t = -\infty$ at the moment of time $t = t_k$ when $G_3(\alpha a_m(t_k)) = 0$. Function $G_2(u)$ has local minimum at $u = u_k = \alpha a_m(t_k)$, and for $t = t_k + \varepsilon$, there is no invariant sphere of radius close to $a_m(t_k)$ because the two neighbouring spheres $\mathbb{B}^3_{a_{2N(t)}}$ and $\mathbb{B}^3_{a_m(t)}$ coincide at $t = t_k$ and then disappear. Therefore, the next ball $\mathbb{B}^3_{a_{2N(t)-1}}$ in the nested sequence (56) becomes maximal. Hence, the radius $a_m(t_k)$ of the vortex blob jumps down to the value $a_{2N(t)-1}(t_k)$ at the moment t_k. The volume $V_m(t) = 4\pi a_m^3(t)/3$ jumps down correspondently. The jumps occur at the moments of time t_k when function

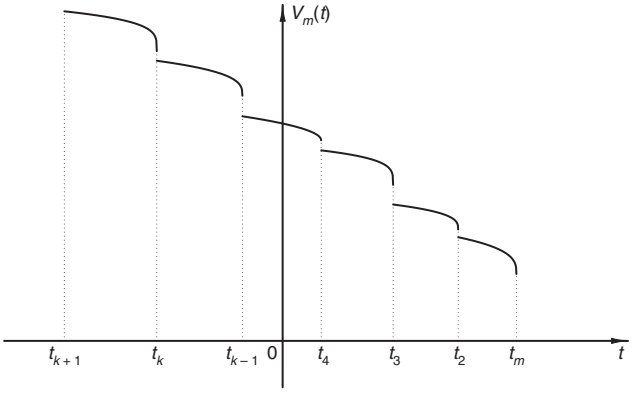

Figure 20: Plot of function $V_m(t)$ for flow (43) with $\xi > 0$.

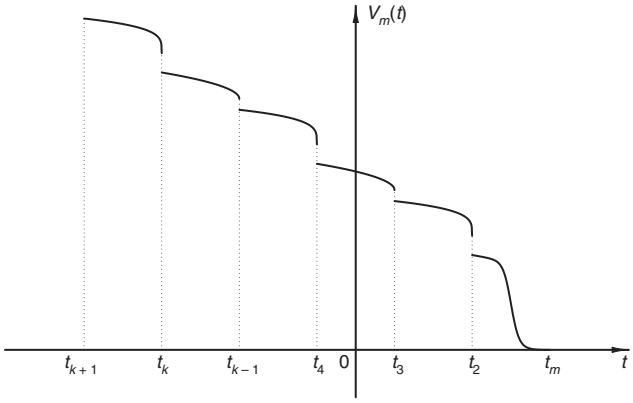

Figure 21: Plot of function $V_m(t)$ for flow (43) with $\xi < 0$.

$G_2(\alpha a_m(t))$ takes the negative values ξ_k (58). The same (61) but with $\xi < 0$ and $\xi_k < 0$ defines the corresponding times t_k.

For $\xi < 0$, we get from (52) that the maximal time $t = t_m^*$ when the flow $\mathbf{V}_1(r, z, t_m^*)$ (43) has a vortex blob $\mathbb{B}^3_{a(t_m^*)}$ is defined by the equation $G_2(\alpha a(t_m^*)) = -1/3 = \min G_2(u)$. Hence, (52) yields the equation for the time t_m^*:

$$\int_0^{t_m^*} \nu(\tau)\mathrm{d}\tau = \alpha^{-2}\log(-1/(3\xi)). \tag{63}$$

The last vortex blob $\mathbb{B}^3_{a(t_m^*)}$ has zero radius $a(t_m^*) = 0$. From (39), we get $G_2(0) = -1/3$, $G_3(0) = 1/15$. Substituting this into (60), we get $\mathrm{d}V_m(t_m^*)/\mathrm{d}t = 0$. Therefore, the plot of function $V_m(t)$ for $\xi < 0$ differs from the plot in Figure 20 for $\xi > 0$ by its behaviour near point t_m^*: the limit values of $V_m(t_m^*)$ and its derivative $\mathrm{d}V_m(t_m^*)/\mathrm{d}t$ are both zeros; see Figure 21.

The fluid flow $\mathbf{V}_1(r, z, t)$ (43) has no vortex blobs and invariant spheres for all times $t > t_m^*$.

8 Conclusion

In this article, we presented an infinite-dimensional space of new exact time-dependent axisymmetric solutions (2) to (6) to the Navier–Stokes equations (1). The solutions are analytic in the whole space $\mathbb{R}^3$ and exist for all times t; the velocity field and vorticity field for the solutions are not collinear and satisfy (11). The constructed space of exact viscous fluid flows $\mathbf{V}(r, z, t)$ is invariant under arbitrary shifts $z \to z + z_0$ and differentiations $\partial^k/\partial z^k$, $k = 1, 2, 3, \cdots$. The iterations of these transforms generate infinite sequences of new exact solutions from any known one.

We studied solutions with velocity field $\mathbf{V}_1(r, z, t)$ (33) having the streamfunction (42):

$$\psi_1(r, z, t) = r^2[\xi - f(t)G_2(\alpha R)],$$

$$f(t) = \exp\left(-\alpha^2 \int_0^t \nu(\tau)\mathrm{d}\tau\right). \qquad (64)$$

Applying transforms (35) to the streamfunction $\psi_1(r, z, t)$, we get an infinite sequence of streamfunctions

$$\psi_n(r, z, t) = r^2\left[\xi - f(t)\frac{\partial^{n-1}G_2(\alpha R)}{\partial z^{n-1}}\right], \qquad (65)$$

that define by formula (33) new exact solutions $\mathbf{V}_n(r, z, t)$ to the Navier–Stokes equations; here, $n = 2, 3, \cdots$. The streamfunctions $\psi_1(r, z, t)$ (64) and $\psi_{2k+1}(r, z, t)$ (65) are up-down symmetric with respect to the reflection $z \to -z$, as well as the corresponding velocity fields (33). The streamfunctions $\psi_{2k}(r, z, t)$ (65) and the related vector fields (33) are up-down asymmetric.

We presented Figures 2–19 describing the bifurcations of the instantaneous (for $t = t_0$) phase portraits of the viscous fluid flows (43). As $t \to \infty$, the derived exact solutions tend to the steady flow $\mathbf{V}(r, z) = \alpha\xi r\hat{\mathbf{e}}_\varphi + 2\xi\hat{\mathbf{e}}_z$ that has a constant vorticity $\nabla \times \mathbf{V}(r, z) = 2\alpha\xi\hat{\mathbf{e}}_z$ and hence has no vortex blobs and vortex rings. Therefore, for the constructed exact solutions to the Navier–Stokes equations, the vortex blobs and vortex rings collapse and disappear as $t \to \infty$.

For the exact fluid flows (43), we studied the behaviour of the volume $V_m(t)$ of the vortex blob. We proved that function $V_m(t)$ is a discontinuous monotonously decreasing function of time t that has jumps down and infinite derivatives at an infinite sequence of moments of time $-\infty < \cdots < t_k < \cdots < t_3 < t_2 < t_m$, where t_m is the maximal time when the vortex blob exists.

References

[1] G. K. Batchelor, An Introduction to Fluid Dynamics, Cambridge University Press, Cambridge 1967.
[2] P. Constantin and C. Foias, Navier–Stokes Equations, The University of Chicago Press, Chicago 1988.
[3] J. C. Mattingly and Ya. G. Sinai, Commun. Contemp. Math. **1**, 497 (1999).
[4] V. L. Fefferman, in: The Millennium Prize Problems (Eds. J. Carlson, A. Jaffe, A. Wiles), Clay Mathematics Institute, Cambridge, Massachusets 2006.
[5] A. J. Majda and A. L. Bertozzi, Vorticity and Incompressible Flow, Cambridge University Press, Cambridge 2002.
[6] C. Y. Wang, Appl. Mech Rev. **42**, 269 (1989).
[7] C. Y. Wang, Acta Mech. **81**, 69 (1990).
[8] C. Y. Wang, Annu. Rev. Fluid Mech. **23**, 159 (1991).
[9] P. G. Drazin and N. Riley, The Navier–Stokes Equations: A Classification of Flows and Exact Solutions, Cambridge University Press, Cambridge 2006.
[10] C. Y. Wang, Eur. J. Mech. B Fluids **30**, 475 (2011).
[11] O. Bogoyavlenskij, C. R. Math. Rep. Acad. Sci. Canada **24**, 138 (2002).
[12] O. Bogoyavlenskij, Phys. Lett. A **307**, 281 (2003).
[13] H. Grad and H. Rubin, in: Proceedings of the Second United Nations International Conference on the Peaceful Uses of Atomic Energy, 31, United Nations, Geneva 1958, p. 190.
[14] V. D. Shafranov, Sov. Phys. JETP **6**, 3 (1958).
[15] W. Heisenberg, in: Hitler's Uranium Club. The Secret Recordings at Farm Hall (Ed. J. Bernstein), American Institute of Physics, Woodbury, New York 1996, pp. 187–209.
[16] W. M. Hicks, Phil. Trans. Roy. Soc. London A **192**, 33 (1899).
[17] W. M. Hicks, P. R. Soc. London **62**, 332 (1898).
[18] O. Bogoyavlenskij, Z. Naturforsch. A **74**, 163 (2019).
[19] G. N. Watson, A Treatise on the Theory of Bessel functions, Cambridge University Press, Cambridge 1980.
[20] S. Chandrasekhar, Proc. Nat. Acad. Sci. **42**, 1 (1956).
[21] L. Woltjer, B. Astron. I. Neth. **14**, 39 (1958).
[22] M. N. Rosenbluth and M. N. Bussac, Nucl. Fusion **19**, 489 (1979).
[23] T. R. Jarboe, Plasma Phys. Contr. F. **36**, 945 (1994).
[24] O. Bogoyavlenskij, J. Math. Anal. Appl. **450**, 21 (2017).
[25] O. Bogoyavlenskij, J. Math. Phys. **58**, 013101 (2017).
[26] O. Bogoyavlenskij, Phys. Rev. E **95**, 043104 (2017).